

Structure and biosynthesis of kendomycin, a carbocyclic *ansa*-compound from *Streptomyces*

1
PERKIN

Helge B. Bode and Axel Zeeck*

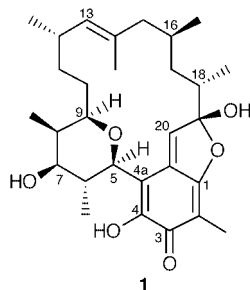
Institut für Organische Chemie, Universität Göttingen, Tammannstr. 2, D-37077 Göttingen, Germany

Received (in Cambridge, UK) 20th October 1999, Accepted 24th November 1999

Kendomycin [(–)-TAN 2162] **1** was re-isolated from *Streptomyces violaceoruber* (strain 3844-33C) in the course of our chemical screening programme. The structure with the relative configuration only was confirmed by the X-ray analysis of **1**. The absolute configuration of **1** was determined by using the advanced Mosher's ester method applied to kendomycin acetonide **2**. The biosynthesis of **1** was performed using stable isotope labelling experiments. From the results it is assumed that a highly oxygenated benzoic acid, derived from (3,5-dihydroxyphenyl)acetic acid, serves as the starter unit of the aliphatic polyketide chain. The cyclisation generating the 18-membered *ansa*-bridge by the formation of a C–C bond might follow a new type of aldol condensation. **1** and **2** exhibit antibacterial activity and strong cytotoxicity against different tumor cell lines.

Introduction

Kendomycin [(–)-TAN 2162] **1** was recently described in the patent literature as a potent endothelin receptor antagonist^{1,2} and antiosteoporotic compound³ produced by two different *Streptomyces* species. We detected **1** in our screening for new metabolites from Actinomycetes. *Streptomyces violaceoruber* (strain 3844-33C) attracted attention by its ability to degrade natural rubber.⁴ By using complex media this strain was striking when its extracts were applied to our chemical screening selection programme.⁵ Kendomycin **1** was isolated from the mycelium (70 mg l⁻¹) following the intensive yellow colour and was identified as (–)-TAN 2162 by comparison of the physico-chemical data. The structure of **1** could be confirmed on the basis of an X-ray analysis in connection with a derivative, to which Mosher's ester methodology⁶ could be applied leading to the absolute configuration. **1** shows an aliphatic *ansa*-chain connected to a unique quinone methide chromophore *via* C–C bonds. While the aliphatic chain obviously originates from a polyketide pathway, the origin of the chromophore and the cyclisation step need to be clarified.



This paper deals with the biogenetic origin of all carbon atoms of kendomycin **1**. The involvement of a chalcone synthase for the biosynthesis of the benzoic acid derivative, which serves as the polyketide starter, the late steps of the biosynthesis and enzymic requirements for the overall biosynthesis are discussed. Furthermore, we present the antibacterial and remarkable cytotoxic properties of **1** and its derivative **2**.

Results

Structure elucidation

The structure and relative stereochemistry of kendomycin **1** was

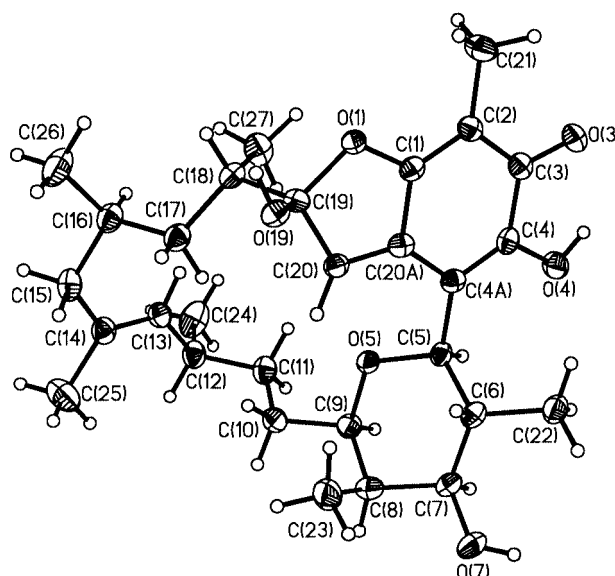


Fig. 1 Perspective view of kendomycin **1**. Only the relative configuration resulted from the X-ray analysis. The given absolute configuration was determined using Mosher's methodology. Crystallographic numbering is shown.

elucidated unambiguously using both extensive 2D-NMR measurements and X-ray analysis of **1**. A tabulation of the ¹³C NMR signal assignment for **1** is given in Table 1. From the data obtained from HMBC and ¹H–¹H COSY experiments we were able to correct the ¹³C NMR assignments in the literature.³ Kendomycin **1** crystallised from a saturated solution in CH₂Cl₂. Fig. 1 shows the crystal structure of **1** from which only the relative configuration of the *ansa*-bridge could be determined. Oxidation of **1** with FeCl₃ in acetone led to the formation of kendomycin acetonide **2** with only one hydroxy group left in the molecule. The advanced Mosher's ester methodology⁶ was used to determine the absolute configuration of C-7 in **2** as *S*, resulting in the absolute configuration of **1**. Table 2 shows selected ¹H NMR shift data of **2** and the Mosher ester derivatives **2a** and **2b**.

Biological activity

Besides the biological activities given in the patent literature¹⁻³

Table 1 Carbon-13 distribution in **1** biosynthesized from labelled precursors. ^{13}C NMR spectra were taken in $[\text{D}_5]\text{pyridine}$ (75.5 MHz)

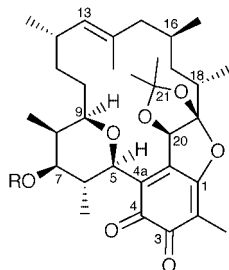
C Atom	δ_{C} (ppm)	[1- ^{13}C]Acetate ^a	[2- ^{13}C]Acetate ^b	[1,2- $^{13}\text{C}_2$]Acetate		[1- ^{13}C]Propionate ^e
				A ^c	B ^d	
1	168.0	8.0	0.3	76.0/48.0	6.1	1.0
2	104.5	0.0	7.0	76.0/60.5	6.8	0.9
3	182.7	7.7	0.3	54.0/60.5	7.5	1.6
4	148.4	0.3	4.4	54.0/80.0	4.4	2.2
4a	111.5	7.3	0.0	62.0/80.0	5.1	0.9
5	77.6	0.1	7.4		10.2	1.1
6	38.2	0.5	4.0		6.7	0.2
7	75.9	3.2	3.4		5.5	38.9
8	40.9	0.4	6.0		6.6	0.3
9	78.4	3.2	2.9		5.3	39.0
10	33.2	0.3	8.0	36.0	10.6	0.6
11	35.5	17.0	0.0	36.0	13.7	1.3
12	33.3	0.4	5.6		5.8	0.3
13	129.6	3.6	3.6		6.3	70.0
14	131.7	0.2	6.3		4.3	0.5
15	45.7	3.4	2.7		5.9	50.2
16	26.2	0.5	4.4		6.2	0.2
17	39.5	4.3	3.6		7.3	52.5
18	41.3	0.4	4.8		5.7	0.7
19	119.5	2.2	2.4		3.7	75.7
20	140.9	0.4	4.1		10.3	0.0
20a	130.2	0.3	5.5	62.0/48.0	7.2	0.9
2-Me	8.2	0.7	0.0		0.0	0.2
6-Me	13.7	1.5	6.2		5.5	0.6
8-Me	7.5	1.2	5.9		5.0	0.9
12-Me	22.8	1.6	5.0		5.1	1.3
14-Me	19.9	1.5	6.5		4.4	1.3
16-Me	19.8	1.4	6.6		3.2	0.0
18-Me	12.8	1.7	6.7		6.3	1.1

^a Relative to the natural abundance of C-4. ^b Relative to the natural abundance of C-4a. ^c $^1J_{\text{C-C}}/\text{Hz}$. ^d Relative to the natural abundance of 2- CH_3 , signal intensity of the multiplet. ^e Relative to the natural abundance of 16- CH_3 .

Table 2 Selected ^1H NMR data for **2** and the Mosher ester **2a** and **2b**, δ_{H} in CDCl_3 (J in Hz)

H Atom	2	2a	2b	$\Delta\delta_{2\text{a} - 2\text{b}}$
5	4.25	4.36	4.34	+0.02
6	1.79	2.02	1.98	+0.04
6- CH_3	0.78	0.69	0.50	+0.19
7	3.51	4.89	4.95	S^a
8	1.85	2.10	2.12	-0.02
8- CH_3	0.91	0.64	0.89	-0.25
9	3.40	3.49	3.51	-0.02

^a Resulting absolute configuration.



2 R = H
2a R = (S)-MTPA
2b R = (R)-MTPA

kandomycin **1** and its derivative **2** show remarkable anti-bacterial activity against Gram-positive and Gram-negative bacteria, especially against multi-resistant *Staphylococcus aureus* (MRSA) strains (e.g., MIC for STA MU50 3.9 and 7.8 μM , respectively). Cytotoxic effects of both compounds were examined against three different tumor cell lines [HMO2 (stomach adenocarcinoma), HEP G2 (hepatocellular carcinoma), and MCF7 (breast adenocarcinoma)] and both exhibit

remarkable cytotoxicity compared with cisplatin and doxorubicin (Table 3).

Biosynthesis

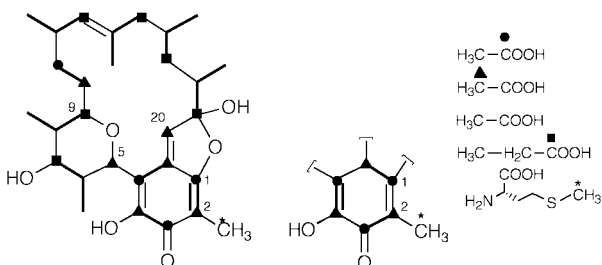
Our working hypothesis for the biosynthesis of **1** envisaged a type I polyketide pathway with the starting unit and the ring-closure mechanism needing to be determined. While the only problem for the aliphatic chain (C-5–C-19) seemed to be the direction of the assembly of propionate and acetate subunits, the origin of the chromophore was more unclear. Possible precursors could be derived *via* polyketide (e.g., 6-methylsalicylic acid⁷) or shikimate pathways (e.g., salicylic acid⁸) followed by additional transformations. Sodium acetate was deemed the best initial precursor for feeding experiments since it had a chance of incorporation into both the aliphatic chain and the chromophore of **1**.

Feeding of [1- ^{13}C]acetate labelled the positions of **1** as depicted in Fig. 2. The enrichment was highest for C-11, followed by C-1, C-3, and C-4a of the chromophore. This pattern is consistent with the polyketide hypothesis as outlined above. Unexpectedly, a weak label was also found in putative propionate-derived positions. Feeding of [1- ^{13}C]propionate results in high enrichments in the carbon atoms C-7, C-9, C-13, C-15, C-17, and C-19 of **1** (Table 1), supporting the notion that the aliphatic methyl groups arise from methylmalonyl-CoA chain-extension units (Fig. 2). Furthermore, these results indicate the direction of the biosynthesis of the aliphatic chain starting at carbon atom C-5 and ending at C-19. To confirm this hypothesis further information about the incorporation of intact acetate moieties was obtained from an experiment with [1,2- $^{13}\text{C}_2$]acetate. Whenever the bond connecting the two isotopes is cleaved during the biosynthesis, metabolic dilution with unlabelled substrate causes a loss of coupling, except for the small amount of coupling introduced by statistical recombination. Only in those instances where there is intact incorpor-

Table 3 Cytotoxic activity of **1** and **2** (in $\mu\text{mol l}^{-1}$)

Compound	HMO2 ^a		HEP G2 ^b		MCF7 ^c	
	GI ₅₀ ^d	TGI ^e	GI ₅₀	TGI	GI ₅₀	TGI
1	<0.1	0.2	<0.1	0.2	<0.1	0.5
2	0.1	0.4	0.8	48	0.2	0.6
Doxorubicin	<0.1	0.1	0.3	1.0	<0.1	0.2
Cisplatin	0.2	1.5	0.5	5.0	0.1	10

^a Stomach adenocarcinoma. ^b Hepatocellular carcinoma. ^c Breast adenocarcinoma. ^d 50% growth inhibition. ^e Total growth inhibition.

**Fig. 2** Labelling pattern of kendomycin **1**.

ation of the precursor will strong spin-spin coupling be observed in the final product. In **1**, we found intact acetate incorporation at C-10/C-11 of the aliphatic chain, confirming the proposed direction of the chain assembly (Fig. 2). As expected, the label was observed in the chromophore as well, showing both possible directions for the biosynthesis of a 6-membered ring from acetate (C-1/C-2, C-3/C-4, C-4a/C-20a and C-1/C-20a, C-4a/C-4, C-3/C-2) as shown in Table 1. Furthermore, we observed labelling of all carbon atoms of **1** except for the C-2-methyl group (Table 1), indicating the involvement of the one-carbon pool in the formation of this methyl branch. To confirm this hypothesis, an experiment with L-[methyl-¹³C]methionine was conducted with **1**. Although there was a drastic inhibitory effect on the biosynthesis of **1**, a high incorporation of label into the C-2-methyl group (77%) could be observed.

In the experiment with [1,2-¹³C₂]acetate we observed a high incorporation of label into carbon atoms C-5 and C-20 of **1** which was not observed in the experiment with [1-¹³C]acetate. These results led us to investigate the biogenetic origin of these two carbon atoms. Feeding of sodium [2-¹³C]acetate resulted in the expected enrichments in carbon atoms C-2, C-4, C-20a, and C-10 but, in addition, also in enrichment of ≈ 7 and 4% of the carbon atoms C-5 and C-20 (Table 1). As observed for the incorporation of [1,2-¹³C₂]acetate, significant enrichments for all carbon atoms derived from methylmalonyl-CoA were observed. It is evident that there was a high degree of turnover of acetate in the citric acid cycle, which gave rise to significant scrambling of the label from [2-¹³C]acetate and [1,2-¹³C₂]acetate, resulting in statistical spin coupling seen in the ¹³C NMR spectrum of **1** as described for the biosynthesis of manumycin.⁹

Discussion

We have presented the absolute configuration and biological activity of the antibiotic kendomycin [(–)-TAN 2162] **1** and its derivative **2**. The mechanism of the formation of **2** proceeds *via* acetalisation of Lewis acid-activated acetone by the hemiacetalic hydroxy group of **1**, followed by nucleophilic attack of the resulting hydroxy group at C-20 and the final oxidation of the catechol intermediate by FeCl₃. This was shown by using dil. hydrochloric acid in acetone for the formation of the catechol and its oxidation with MnO₂ on an analytical scale (data not shown). The high electrophilicity of the carbon atom C-20 might be the main reason for the high cytotoxicity of **1** due to its ability to react with numerous biological nucleophiles

(e.g. enzymic thiol groups or amino functions of DNA) similar to the reaction of CC-1065 with DNA¹⁰ but does not explain the high cytotoxicity of **2**. Further experiments to identify the biological target and to elucidate the mechanism of action are in progress.

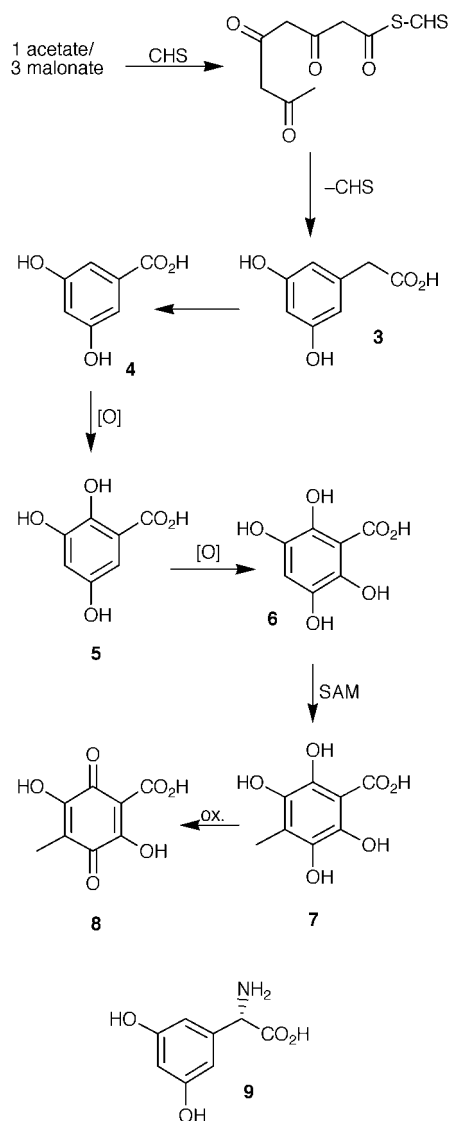
In combination, the results of our feeding experiments of ¹³C-labelled precursors to *S. violaceoruber* (strain 3844-33C) have provided a nearly complete picture of the biosynthetic origin of **1**, which is a product of a bacterial type-I polyketide synthase (PKS I) with both an unusual starter unit and a so-far-unknown termination step.

The starter unit is derived from acetate and methionine only. At this point we can only speculate that 3,5-dihydroxybenzoic acid **4** (Scheme 1) serves as the starter directly and is modified later or if acid **4** is modified prior to serving as the starter unit. Biosynthetic considerations led us to propose a second possibility due to the ring-closure mechanism described below. The incorporation pattern in the chromophore gave evidence for (3,5-dihydroxyphenyl)acetic acid **3** as the first intermediate derived from a chalcone synthase (CHS), excluding a shikimate pathway. Chalcone synthases are well known enzymes in plant secondary metabolism¹¹ but increasing research in bacterial secondary metabolism gives evidence for CHSs being present in at least some *Streptomyces* species^{12,13} and involved in the biosynthesis of various secondary metabolites. In the gene cluster of the glycopeptide antibiotic chloroeremomycin,¹⁴ for example, a CHS was found and (3,5-dihydroxyphenyl)glycine **9**, the analogous amino acid of **3**, is part of the peptide backbone.

In our strain **3** must be oxidatively decarboxylated to give **4** that might act as the starter unit. From the incorporation of [1,2-¹³C₂]acetate with both possible directions of the biosynthesis observed we must assume a symmetrical intermediate at least before the ring-closure step takes place. The most likely compound that needs no further modifications for the ring-closure step is the highly substituted acid **8** but even compounds **5**, **6** or **7** might be the starter unit and be modified in the later stages of biosynthesis. Anyway, the enzyme system required for the biosynthesis of **8** is rather complex. At least the involvement of a chalcone synthase, a decarboxylase, a methyl transferase, and one or more oxidases can be predicted.

No matter what the starter unit is exactly, the following steps are typical for a type-I PKS. Six methylmalonyl-CoA and two malonyl-CoA molecules are needed to build up the aliphatic chain. From detailed investigations of various type-I PKSs¹⁵⁻¹⁷ we can propose the presence of eight modules and one loading domain with different enzymic activities. Furthermore, the formation of the pyran ring between C-5 and C-9 would require a reductive cyclisation.

Usually the last step in the biosynthesis of type-I polyketides involves a thioesterase (TE) that cyclises the enzyme-bound chain to give the first free intermediate *via* the formation of a macrolactone.¹⁸ The label obtained after feeding sodium [2-¹³C]acetate led us to propose a ring-closure mechanism as shown in Scheme 2 similar to the aldol condensation found during chain extension in fatty acid and polyketide biosynthesis. TE-mediated cleavage of the enzyme-polyketide complex results in the putative intermediate **10** that is cyclised to the pyran structure **11**. Decarboxylation of **11** led to the



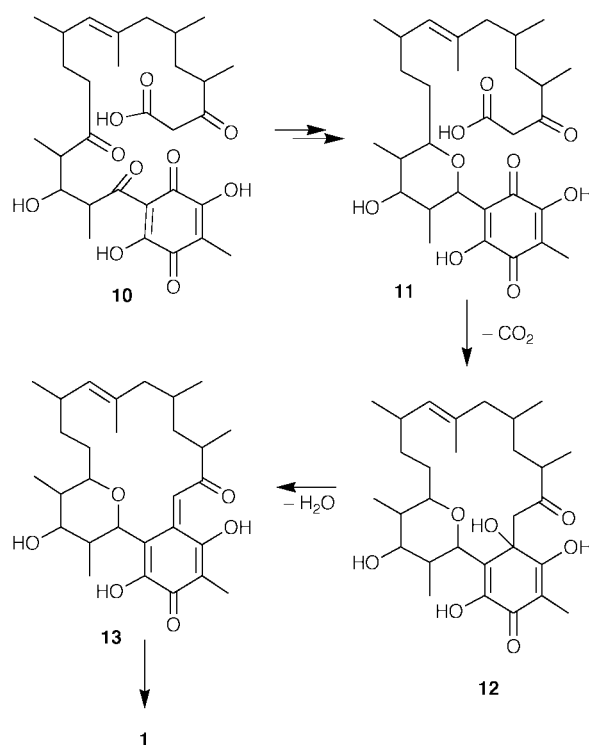
Scheme 1 Biosynthesis of the starter unit.

formation of a carbanion that could attack one carbonyl carbon of the starter quinone regioselectively. The resulting intermediate **12** would eliminate water almost spontaneously to give **13**. Hemiacetal formation between the hydroxy group at C-1 and the carbonyl group at C-19 would result in **1** as depicted in Scheme 2.

Experimental

General

*Streptomyces violaceoruber*⁴ (strain 3844-33C) was obtained from Dr D. Jendrossek, Universität Stuttgart, Germany. All materials are of analytical or HPLC grade. Sodium [1-¹³C]-acetate and L-[methyl-¹³C]methionine were obtained from Chemotrade, sodium [2-¹³C]-, and [1,2-¹³C₂]acetate from Campro Scientific, and sodium [1-¹³C]propionate was obtained from Cambridge Isotopes. The enrichment of all stable isotopes was 99%. Malt extract was purchased from Merck, yeast extract from Gibco BRL, and degreased soybean meal from Heuselwerk Magstadt. TLC was performed on silica gel plates (Merck, HPTLC ready-to-use plates, silica gel 60 F₂₄₅ on aluminium foil or glass), and column chromatography on silica gel ICN SiliTech 32-63 (0.032–0.063 mm, ICN Biomedicals GmbH) or Sephadex LH-20 (Pharmacia). Physical data for the described compounds were recorded using the following equipment: Mp (Reichert hot-stage microscope, uncorrected values), IR (Perkin-Elmer 298 spectrometer), UV (Varian Cary 3E spectro-



Scheme 2 Ring-closure mechanism of kendomycin biosynthesis.

photometer), optical rotation (Perkin-Elmer 343) ($[\alpha]_D$ -values are in $10^{-1} \text{ deg cm}^2 \text{ g}^{-1}$), CD (JASCO J 500 spectrometer), EI-MS (Varian 311 A, 70 eV, direct insert, high resolution with perfluorokerosine as standard). ¹³C and ¹H NMR spectra were recorded at 295 K on Bruker AMX 300 (¹H 300 MHz, ¹³C 75.5 MHz), Varian Unity 300 (¹H 300 MHz, ¹³C 75.5 MHz), and Varian Inova 500 (¹H 500 MHz, ¹³C 125.7 MHz) spectrometry. Chemical shifts are expressed in δ -values (ppm) using the solvent as internal reference (CDCl₃: $\delta_{\text{H}} = 7.24$, $\delta_{\text{C}} = 77.0$; [D₅]-pyridine: $\delta_{\text{H}} = 8.71$, $\delta_{\text{C}} = 149.9$).

Fermentation

S. violaceoruber (3844-33C) was stored in liquid nitrogen. For production of kendomycin **1** and biosynthetic studies the strain was grown on slants of medium A (soybean meal 2%, mannitol 2%, agar 1.5%, deionised water, pH = 7.0 prior to sterilisation), which were incubated at 28 °C for 4–6 days. For fermentation the following two-stage protocol was used: A 1 cm² piece of agar was used to inoculate 100 ml of medium B (medium A omitting agar) in 300 ml Erlenmeyer flasks with three intrusions. These cultures were cultivated in a rotary shaker (250 rpm) at 28 °C for 2 days. For production of high amounts of **1** the second stage was used to inoculate 60 × 250 ml of medium B in 1 l Erlenmeyer flasks (10% inoculum). Cultures were incubated at 28 °C on a unidirectional shaker (Universität Göttingen) for 72 h. For biosynthetic studies 50 ml of the seed culture was used to inoculate the 1 l fermentor [Braun Biostat B; 1000 ml of medium C (malt extract 1%, yeast extract 0.4%, glucose 0.4%, deionised water, pH = 7.0 prior to sterilisation), aeration 5.0 l min⁻¹] and the culture was harvested after 36 h.

Feeding experiments with labelled precursors

Feeding experiments were carried out under the conditions described above. In general, precursors were administered to the fermentation during 24–30 h. Precursors were added as sterile aqueous solutions, adjusted to pH 7.0, in the amounts indicated: Sodium [1-¹³C]acetate, 10.0 mmol l⁻¹; sodium [2-¹³C]acetate, 11.9 mmol l⁻¹; sodium [1,2-¹³C₂]acetate, 5.6 mmol l⁻¹; sodium [1-¹³C]propionate, 4.9 mmol l⁻¹; L-[methyl-¹³C]methionine, 1.5 mmol l⁻¹.

Isolation and purification

The fermentation broth was centrifuged at 3300 rpm for 30 min, and the supernatant was discarded. The mycelial pellet was treated repeatedly with acetone until extraction of **1** was complete, and the extracts were pooled. After evaporation of acetone, the remaining aqueous residue was lyophilised. Extracts from the biosynthesis experiments were chromatographed twice on a Sephadex LH-20 (Pharmacia) column (100 × 2.5 cm; acetone). The yield of **1** after purification averaged 8 mg l⁻¹. The crude product from the large scale production of **1** was extracted with CH₂Cl₂ in a Soxhlet extractor for 6 h. After evaporation of the solvent the residue was filtered using a short silica gel column (10 × 5 cm; CH₂Cl₂). The filtrate was discarded and **1** was eluted with ethyl acetate. After evaporation of the solvent the crude extract (5.0 g) was crystallised from 20 ml of CH₂Cl₂ at 4 °C to yield 1.25 g of crude **1**. The mother liquid was concentrated and the residue was subjected to silica gel chromatography [20 × 5 cm; CH₂Cl₂–MeOH (16:1)]. Fractions containing **1** (200 mg) were pooled and added to the crude crystals. Recrystallisation of this fraction from CH₂Cl₂, followed by chromatography on Sephadex LH-20 (see above) in 200–300 mg portions, yielded 1.05 g pure **1** (70 mg l⁻¹).

Biological activity

The cytotoxicity tests were carried out according to the NCI standard¹⁹ with the following tumor cell lines: HMO2 (stomach adenocarcinoma), HEP G2 (hepatocellular carcinoma), and MCF7 (breast adenocarcinoma). Cells were cultivated in 96-well plates in RPMI 1640 medium containing 10% fetal calf serum. Compounds **1** and **2** (both dissolved in DMSO or MeOH) were added 24 h after inoculation (*c* = 0.1, 0.5, 1.0, 5.0, 10.0, and 50.0 μmol l⁻¹) and the cells were incubated for an additional 48 h. Cells were counted by determination of the protein content with sulforhodamin. The overall DMSO/MeOH concentration in the assay was 1%.

Kendomycin (5R,6R,7S,8R,9R,12S,13E,16S,18S,19S)-6,7,8,9,10,11,12,15,16,17,18,19-dodecahydro-4,7,19-trihydroxy-2,6,8,12,14,16,18-heptamethyl-1,19:5,9-diepoxybenzo[18]annulene-3(5H)-one **1**

Yellow powder; mp 258 °C; [α]_D²⁰ –80 (*c* 2.71, MeOH), (Found: C, 71.9; H, 8.9. Calc. for C₂₉H₄₂O₆: C, 71.8; H, 8.7%); ν_{\max} (KBr)/cm⁻¹ 3360 (OH), 1666 (C=O), 1611 (C=C), and 1573 (C=C); *m/z* (EI) 486 (M⁺, 91%), 468 ([M – H₂O]⁺, 85), 450 ([M – 2H₂O]⁺, 25), 193 (100) [*m/z* (HREI) Found: M⁺, 486.2981. Calc. for C₂₉H₄₂O₆: *M*, 486.2981]; λ_{\max} /nm (*c* 0.013 35 in CH₃CN) 307 (log ϵ 4.40), 364sh (2.58); λ_{\max} /nm (CH₃CN + HCl) 307 (4.38), 373sh (2.78); λ_{\max} /nm (CH₃CN + NaOH) 306 (4.11), 341sh (3.29), 551 (2.84); CD λ /nm (*c* 0.013 35 in CH₃CN) 228 (θ –3815), 251 (–3307), 305 (41 463), 335 (–23 342); δ_{H} (300 MHz; [D₅]pyridine) 7.53 (s, 20-H), 4.86 (d, *J* = 10.5 Hz, 5-H), 4.81 (d, *J* = 10.0 Hz, 13-H), 3.86 (dd, *J* = 10.0, 4.5 Hz, 7-H), 3.58 (d, *J* = 11.0 Hz, 9-H), 2.78 (m, 18-H), 2.39 (m, 12-H), 2.20 (s, 2-CH₃), 2.12 (d, *J* = 17.0 Hz, 15-H^a), 2.11–2.00 (m, 8-H), 2.05–1.95 (m, 16-H), 1.85 (m, 6-H/17-H₂), 1.67 (m, 10-H^a/15-H^b), 1.65 (s, 14-CH₃), 1.50 (m, 11-H^a), 1.30 (m, 11-H^b), 1.27 (d, *J* = 7.0 Hz, 6-CH₃), 1.20 (m, 10-H^b), 1.18 (d, *J* = 7.0 Hz, 8-CH₃), 1.00 (d, *J* = 7.0 Hz, 12-CH₃), 0.96 (d, *J* = 7.0 Hz, 16-CH₃), 0.93 (d, *J* = 7.0 Hz, 18-CH₃); δ_{H} (500 MHz; [D₆]acetone) 8.10 (s, 4-OH), 7.19 (s, 20-H), 6.54 (s, 19-OH), 4.63 (d, *J* = 9.0 Hz, 13-H), 4.35 (d, *J* = 10.0 Hz, 5-H), 3.95 (d, *J* = 4.5 Hz, 7-OH), 3.56 (dt, *J* = 10.0, 4.5 Hz, 7-H), 3.52 (ddd, *J* = 11.0, 2.0, 1.0 Hz, 9-H), 2.41 (m, 18-H), 2.35 (m, 12-H), 2.12 (m, 15-H^a), 1.96 (m, 16-H), 1.88 (m, 8-H), 1.84 (s, 2-CH₃), 1.70 (m, 6-H), 1.65 (m, 15-H^b), 1.62 (m, 17-H^a), 1.60 (s, 14-CH₃), 1.57 (m, 10-H₂), 1.45 (ddd, *J* = 13.0, 11.0, 3.0 Hz, 17-H^b), 1.32 (m, 11-H^a), 1.25 (m, 11-H^b),

0.95 (d, *J* = 7.0 Hz, 8-CH₃), 0.94 (d, *J* = 7.0 Hz, 16-CH₃), 0.88 (d, *J* = 7.0 Hz, 6-CH₃), 0.86 (d, *J* = 7.0 Hz, 12-CH₃), 0.71 (d, *J* = 7.0 Hz, 18-CH₃); δ_{C} (75.5 MHz; [D₅]pyridine) see Table 1; δ_{C} (125.7 MHz; [D₆]acetone) 182.1 (C-3), 168.6 (C-1), 146.8 (C-4), 141.4 (C-20), 132.1 (C-14), 130.2 (C-20a), 129.9 (C-13), 119.1 (C-19), 111.0 (C-4a), 104.2 (C-2), 78.7 (C-9), 77.7 (C-5), 76.3 (C-7), 46.1 (C-15), 41.4 (C-18), 40.8 (C-8), 39.7 (C-17), 38.1 (C-6), 35.8 (C-11), 33.6 (C-12), 33.4 (C-10), 26.5 (C-16), 22.7 (12-CH₃), 19.9 (14-CH₃), 19.7 (16-CH₃), 13.3 (6-CH₃), 12.7 (18-CH₃), 7.6 (2-CH₃), 7.2 (8-CH₃).

X-Ray crystallography of kendomycin **1**²⁰

Kendomycin **1** was crystallised from a saturated solution in CH₂Cl₂. Crystal data: C₂₉H₄₂O₆, *M* = 486.63, orthorhombic, *P*2₁2₁2₁, *a* = 1003.2(2), *b* = 1090.0(2), *c* = 2477.9(5) pm, *a* = *b* = *c* = 90°, *V* = 2.7094(9) nm³, *Z* = 4, *D*_{calc.} = 1.193 Mg m⁻³, *F*(000) = 1056, μ = 0.082 mm⁻¹. Stoe–Siemens–Huber four-circle-diffractometer coupled to a Siemens CCD-area detector with graphite-monochromated Mo-K α radiation (λ = 0.710 73), –140 °C, θ -range = 4–55°, 37 995 reflections measured, 6247 unique. Structure solved by direct methods using SHELXS-97²¹ and refined against *F*² on all data by full-matrix least-squares with SHELXL-97.²² A riding model with idealised hydrogen geometry was employed, the anisotropic refinement converging at *R*₁ = 0.0441 for *F* > 2 σ (*F*) and *wR*₂ (*F*²) = 0.0925 for all reflections.

Formation of acetone **2** from kendomycin **1**

1 (56 mg) was dissolved in 5 ml of acetone and FeCl₃ was added to the solution in excess (48 mg). After stirring of the mixture for 5 min, water (3 ml) was added and the acetone was evaporated off. The resultant aqueous solution was extracted with ethyl acetate (2 × 100 ml), and the combined organic phases were dried over sodium sulfate, and evaporated to dryness. Chromatography on silica gel [30 × 1 cm; CHCl₃–MeOH (9:1)] yielded **2** as a red amorphous powder (16 mg, 26%). Acetone **2** had mp 107 °C; [α]_D²⁰ –68 (*c* 0.177, MeOH); ν_{\max} (KBr)/cm⁻¹ 3437 (OH), 1684 (C=O), and 1623 (C=C); *m/z* (EI) 542 (M⁺, 15%), 514 ([M – CO]⁺, 90) [*m/z* (HREI) Found: M⁺, 542.3243. C₃₂H₄₆O₇ requires *M*, 542.3244]; λ_{\max} /nm (*c* 0.01575 in CH₃CN) 289 (log ϵ 3.24), 461 (2.02); λ_{\max} /nm (CH₃CN + HCl) 291 (3.33), 461 (2.20); λ_{\max} /nm (CH₃CN + NaOH) 286sh (3.32), 456 (32.25); CD λ /nm (*c* 0.01575 in CH₃CN) 209 (θ 23 761), 282 (–2939), 493 (2645); δ_{H} (300 MHz; CDCl₃) 5.89 (s, 20-H), 4.62 (d, *J* = 9.5 Hz, 13-H), 4.24 (d, *J* = 10.0 Hz, 5-H), 3.51 (dd, *J* = 10.5, 4.5 Hz, 7-H), 3.39 (dd, *J* = 10.0, 2.0 Hz, 9-H), 2.44 (m, 18-H), 2.30 (m, 12-H), 2.13 (m, 15-H^a), 1.94 (m, 16-H), 1.85 (s, 2-CH₃), 1.82 (m, 8-H), 1.79 (m, 6-H), 1.60 (m, 15-H^b), 1.58 (s, 14-CH₃), 1.52 (m, 11-H^a), 1.48, 1.42 (s, 2 × 21-CH₃), 1.47 (m, 10-H^a), 1.32 (m, 17-H^a), 1.25 (m, 10-17-H^b), 1.20 (m, 11-H^b), 0.94 (d, *J* = 7.0 Hz, 16-CH₃), 0.90 (d, *J* = 7.0 Hz, 8-CH₃), 0.87 (d, *J* = 7.0 Hz, 18-CH₃), 0.83 (d, *J* = 7.0 Hz, 12-CH₃), 0.78 (d, *J* = 7.0 Hz, 6-CH₃); δ_{C} (75.5 MHz; CDCl₃) 179.5 (C-4), 177.8 (C-3), 164.9 (C-1), 145.9 (C-4a), 136.6 (C-20a), 131.6 (C-14), 129.0 (C-13), 123.9 (C-19), 115.9 (C-21), 109.9 (C-2), 78.4 (C-9), 76.6 (C-7), 75.5 (C-5), 75.1 (C-20), 45.2 (C-15), 39.7 (C-8), 38.7 (C-6), 37.3 (C-11), 35.3 (C-17), 35.2 (C-18), 32.8 (C-12), 32.7 (C-10), 28.0, 27.0 (2 × 21-CH₃), 25.6 (C-16), 22.4 (18-CH₃), 20.0 (16-CH₃), 19.5 (14-CH₃), 13.4 (12-CH₃), 12.8 (6-CH₃), 7.9 (2-CH₃), 5.9 (8-CH₃).

Preparation of Mosher's ester⁵

To 5 mg of **2** in 1.5 ml of CH₂Cl₂ were sequentially added 0.2 ml of pyridine, 4 mg of 4-(dimethylamino)pyridine and 20 mg of (*R*)-(–)- α -methoxy- α -(trifluoromethyl)phenylacetyl chloride [(*R*)-MTPA-Cl]. The mixture was stirred overnight at room temperature, checked with TLC to make sure that the reaction was complete, and passed through a disposable pipette (0.4 × 5

cm) containing silica gel (ICN Silica 32–63) and eluted with 10 ml of CH₂Cl₂. The red residue was dried *in vacuo* and subjected to a second chromatography step identical to the first one to give the (*S*)-MTPA Mosher ester **2a** (5 mg). Using (*S*)-(+)- α -methoxy- α -(trifluoromethyl)phenylacetyl chloride gave the (*R*)-MTPA Mosher ester **2b** (5 mg). The structure of both derivatives was confirmed by 2D NMR measurements and mass spectroscopy (*m/z* [HREI] Found: M⁺, 758.3641. C₄₂H₅₃F₃O₉ requires *M*, 758.3642 for **2a** and **2b**). For partial ¹H NMR assignments of **2a** and **2b** see Table 2.

Acknowledgements

We are grateful to Dr D. Jendrossek (Technische Universität Stuttgart) for providing us with the strain, to Dr M. Walker (Universität Göttingen) for performing the X-ray analysis, to Professor W. Beil (Medizinische Hochschule Hannover) for determining the cytotoxic activity and to Professor H. Labischinski (Bayer AG, Wuppertal) for performing the STA-tests. Part of this work was financed by a grant from the Deutsche Forschungsgemeinschaft (Graduiertenkolleg 227).

References

- 1 Y. Funahashi, N. Kawamura and T. Ishimaru, *Jap. Pat.* 08 231 551 [A2 960 910], 1996 (*Chem. Abstr.*, 1997, **126**, 6553).
- 2 Y. Funahashi, T. Ishimaru and N. Kawamura, *Jap. Pat.* 08 231 552 [A2 960910], 1996 (*Chem. Abstr.*, 1996, **125**, 326518).
- 3 M. H. Su, M. I. Hosken, B. J. Hotovec and T. L. Johnston, *US Pat.* 5 728 727 [A 9803 17], 1998 (*Chem. Abstr.*, 1998, **128**, 239489).
- 4 D. Jendrossek, G. Tomasi and R. M. Kroppenstedt, *FEMS Microbiol. Lett.*, 1997, **150**, 179.
- 5 S. Grabley, R. Thiericke and A. Zeeck, in *Drug Discovery from Nature*, ed. S. Grabley and R. Thiericke, Springer, Berlin-Heidelberg, 1999, pp. 124–148.
- 6 M. J. Rieser, Y. H. J. K. Rupprecht, J. F. Kozlowski, K. V. Wood, J. L. McLaughlin, P. R. Hanson, Z. Zhuang and T. R. Hoye, *J. Am. Chem. Soc.*, 1992, **114**, 10203.
- 7 J. Beck, S. Ripka, A. Siegner, E. Schiltz and E. Schweizer, *Eur. J. Biochem.*, 1990, **192**, 487.
- 8 P. M. Dewick, *Nat. Prod. Rep.*, 1998, **15**, 17.
- 9 R. Thiericke, A. Zeeck, A. Nakagawa, S. Omura, R. E. Herrold, S. T. S. Wu, J. M. Beale and H. G. Floss, *J. Am. Chem. Soc.*, 1990, **112**, 3979.
- 10 D. L. Boger and D. S. Johnson, *Angew. Chem.*, 1996, **108**, 1542; *Angew. Chem., Int. Ed. Engl.*, 1996, **35**, 1438.
- 11 J. Schröder, in *Comprehensive Natural Products Chemistry*, ed. U. Sankawa, Elsevier, Amsterdam, 1999, vol. 1, 749.
- 12 N. Funa, Y. Ohnishi, I. Fujii, M. Shibuya, Y. Ebizuka and S. Horinouchi, *Nature*, 1999, **400**, 897.
- 13 K. Shin-ya, K. Furihata, Y. Hayakawa and H. Seto, *Tetrahedron Lett.*, 1990, **31**, 6025.
- 14 A. M. A. van Wageningen, P. N. Kirkpatrick, D. H. Williams, B. R. Harris, J. K. Kershaw, N. J. Lennard, M. Jones, S. J. M. Jones and P. J. Solenberg, *Chem. Biol.*, 1998, **5**, 155.
- 15 J. Staunton and B. Wilkinson, *Chem. Rev.*, 1997, **97**, 2611.
- 16 C. Khosla, *Chem. Rev.*, 1997, **97**, 2577.
- 17 D. A. Hopwood, *Chem. Rev.*, 1997, **97**, 2465.
- 18 A. R. Butler, N. Bate and E. Cundliffe, *Chem. Biol.*, 1999, **6**, 287.
- 19 M. R. Grever, S. A. Schepartz and B. A. Chabner, *Semin. Oncol.*, 1992, **19**, 622.
- 20 CCDC reference number 207/381. See <http://www.rsc.org/suppdata/p1/a9/a908387a> for crystallographic files in .cif format.
- 21 G. M. Sheldrick, *Acta Crystallogr., Sect. A*, 1990, **46**, 467.
- 22 G. M. Sheldrick, *SHELXL-97*, Universität Göttingen, 1997.

Paper a908387a